Available online at www.sciencedirect.com
ScienceDirect
Journal of Power Sources 165 (2007) 559–565
JOURNAL OF POWER SOURCES
www.elsevier.com/locate/jpowsour

Development and utility of manganese oxides as cathodes in lithium batteries

Christopher S. Johnson *

Electrochemical Technology Program, Chemical Engineering Division, Argonne National Laboratory, Argonne, IL 60439, USA

Available online 13 November 2006

Abstract

Manganese oxides have a long history of serving as a cathode in charge storage applications. Electrolytic manganese dioxide (EMD) is widely used in alkaline batteries and MnO_2 originally was part of the Leclanché wet cell patented in 1866. Leclanché wet cells used a naturally occurring MnO_2 ore with Zn metal as anode and ammonium chloride electrolyte. While there are a vast number of topics to discuss on manganese oxides, in this short paper, two topics researched at Argonne over the last 12 years are highlighted. First, the addition of lithia (Li_2O) as a stabilizing component in 3 V alpha-MnO_2 is examined. Second, an overview of the evolution of layered–layered composite-structured electrodes derived from the lithium-manganese oxide (Li_2MnO_3) layered rock-salt phase is presented.
© 2006 Elsevier B.V. All rights reserved.

Keywords: Lithium battery; Composite electrode; Alpha-MnO_2; Manganese oxide; Li_2MnO_3

1. Introduction

1.1. Why MnO_2?

The primary driving force for implementation of MnO_2-based materials for battery applications is the cost. Roughly, raw material cost to synthesize MnO_2 materials is about 1% the cost of Co raw materials. Therefore, a MnO_2 positive electrode material or cathode or lithiated MnO_2 cathode would be projected to cost 1% of $LiCoO_2$, the cathode material of choice in rechargeable Li-ion batteries. Essentially, properties such as cycle life and operation voltage and energy density may be secondary issues for MnO_2 materials when compared to $LiCoO_2$ due to the potential cost difference. From a rechargeable battery business standpoint, one can, in effect, sell more MnO_2 type batteries as replacements for an application after the performance has degraded which is an attractive feature.

Other desirable features of MnO_2 materials are an increased safety margin to over-charge conditions compared to Co or Ni based Li-ion batteries. This is due to the stable nature of Mn(IV), which is a common oxidation state for Mn and one that retains oxygen. Thermodynamically, MnO_2 is the most stable form for a manganese-oxygen compound at standard temperature and oxygen pressure [1], whereas Co(IV) and Ni(IV) that represent the oxidation state of $Li_{1-x}CoO_2$, $Li_{1-x}NiO_2$, or $Li_{1-x}Co_{1-y}Ni_yO_2$ at top of charge ($x \sim 1$) are thermally unstable [2]. This in essence makes Co(IV) and Ni(IV) more dangerous in an over-charge condition, particularly when the material is combined with an organic-based (flammable) electrolyte and carbon anode in a cell which can burn.

Manganese is also an abundant transition metal. It is the 12th most abundant element in the earth's crust. Only the transition metals Ti and Fe are present in larger quantities [3]. For this reason, a significant infrastructure for the use of Mn-based cathodes can be envisioned. Therefore, MnO_2 type materials are attractive for large energy storage applications like electric vehicles (EVs) and hybrid electric vehicles (HEVs), which would require very large quantities of materials to supply an emerging market. The use of MnO_2 as the cathode in alkaline batteries produced worldwide underscores the abundant quantities of raw materials available for use.

MnO_2 is regarded as non-toxic and a common material. As stated earlier, it is used in cathodes of primary alkaline batteries. The consumer presently discards spent primary alkaline batteries in the garbage, so MnO_2 enjoys a comfort level in this respect. MnO_2 materials are versatile. Product lines from alkaline batteries to lithium batteries and to even supercapacitors are possible from MnO_2 based materials.

* Tel.: +1 630 252 4787; fax: +1 630 252 4176.
E-mail address: johnsoncs@cmt.anl.gov.

0378-7753/$ – see front matter © 2006 Elsevier B.V. All rights reserved.
doi:10.1016/j.jpowsour.2006.10.040

Table 1
Energy densities of Li/MnO_2 cells

Structure type	Average discharge voltage (V)	x range	Theoretical capacity (mAh g^{-1})	Practical capacity (mAh g^{-1})	% Electrode utilization	Li per Mn	Energy density (Wh kg^{-1})
$Li_xMn_2O_4$ spinel	4.0	$0 \le x \le 1$	148	110–120	81	0.4	480
Li_xMnO_2	2.8 (3.0)	$0 \le x \le 1$	308	160–180	58	0.6	504

1.2. MnO_2 themes

There are three themes that MnO_2 materials adhere to. First, MnO_2 can be stabilized by lithia (Li_2O) addition to the structure. Addition of Li_2O adds lithium cations and additional oxygen into the structure, thereby imparting structural stability which aids the material to allow lithium insertion and extraction [4]. Secondly, acid-treatment of $xLi_2O{\cdot}yMnO_2$ materials can remove or control the Li_2O content in the structure. Tetravalent Mn(IV) is stable in acid, but Li_2O is soluble in acid and thus dissolves away from the matrix. Such reactions can change the nature of the MnO_2 material. Third, MnO_2 materials may adopt many polymorphic structures with various MnO_6 octahedral bonding arrangements. This property allows the formation of composites or intergrowths of materials and, as a result, a host of structures may be accommodated.

Finally, it is worth noting that the International Battery Materials Association, Inc. (IBA, Inc.) is an organization that was created to promote and share common understanding of battery materials [5]. This association can trace its roots to Union Carbide in Parma, Ohio, a suburb of Cleveland, Ohio, where Dr. Akiya Kozawa first established an international common sample database for MnO_2 battery materials in 1970. In 1983, while Dr. Kozawa worked at Eveready (Westlake, Ohio), the IBA was officially formed, with Dr. Kozawa serving as its first Chairman.

2. Results and discussion

2.1. Energy densities of Li/MnO_2 cells

Manganese oxides can be broken down into three areas related to their use as cathodes in lithium batteries. First, the spinel $LiMn_2O_4$ is a 3-dimensional framework structure that allows transport of lithium cations in tetrahedral interstitial sites [6]. This process has a nominal voltage of 4 V versus metallic Li. The second class includes 3 V MnO_2 electrode materials [7] that can be either primary or secondary cathode materials. These materials consist mostly of compounds such as alpha-MnO_2 (α-MnO_2; 2×2 tunnels), r-MnO_2 (ramsdellite, 2×1 tunnels), and a heat-treated version of γ-MnO_2 (electrolytic manganese dioxide or EMD; intergrowth of pyrolusite (1×1 tunnels) and ramsdellite) that has been commercialized for lithium batteries [8]. The mechanism of lithium insertion into γ-MnO_2 has been studied by Ohzuku et al. [9]. Pyrolusite and ramsdellite are naturally occurring minerals of MnO_2. The structures of these minerals are composed of MnO_6 octahedra which share edges and/or corners to form a framework structure containing tunnels of different size. Ramsdellite-MnO_2 slowly converts to spinel with cycling [10], and pyrolusite or β-MnO_2 with its 1×1 tunnels may be to constrictive for Li cation insertion, although it has been reported that nanocrystals of β-MnO_2 are topotactically active to Li insertion on the first discharge, but convert to spinel $LiMn_2O_4$ with cycling in lithium cells [11]. The operational voltage is lower than spinel primarily because the coordination of Li upon discharge in these materials is octahedral and, as a consequence, the reaction occurs at lower voltages.

Lithium has also been introduced by reaction of EMD in organic media to form reduced lithiated MnO_2 phases [12], or by reaction of γ-MnO_2 with a lithium salt mixture to form composite dimensional manganese oxide (CDMO) [13]. Also reported recently is a lithium-cation exchanged EMD product [14]. Various lithium containing 3 V MnO_2 materials related to orthorhombic $LiMnO_2$ have also been examined [15].

The third class of MnO_2 cathodes for lithium batteries is comprised of layered $LiMnO_2$ and related layered Li_2MnO_3. Layered $LiMnO_2$ slowly converts to spinel on cycling [16] but Li_2MnO_3 affords an opportunity to use the phase as a stabilizing component in composite-structured electrodes [17,18]. Interestingly, Li_2MnO_3 traditionally has been viewed as an unwanted "inactive" phase and considered undesirable for electrodes. The voltage of operation can vary from 1.5 V to around 4.5 V depending on the layered material and whether the lithium site involves an octahedral or tetrahedral interstitial.

Table 1 breaks down the comparison of energy densities of MnO_2 materials. In this table spinel 4 V $LiMn_2O_4$ is compared with 3 V Li_xMnO_2 type materials. Because a higher theoretical and practical capacity is possible with 3 V MnO_2 materials, the energy densities of cells based on either material is roughly equivalent. About 504 Wh kg^{-1} may be realized with 3 V Li_xMnO_2 cells, while the spinel offers about 480 Wh kg^{-1}. Of course other factors, such as whether the material is in an initial charged or discharged state, are important as well as the tap density, but one can expect equivalent stored energy on a weight-basis in both systems.

2.2. Development of alpha-MnO_2 materials

At Argonne National Laboratory in the early to mid 1990s, a joint research and development project to evaluate and test Li-polymer cells was created. This project was funded as a Cooperative Research and Development Agreement (CRADA) with 3 M Corp. and Hydro-Quebéc and was sponsored by the United States Advanced Battery Consortium (USABC) and U.S. Department of Energy (DOE). The electrolyte in the Li-polymer cell was unique. It consisted of a dry poly(ethyleneoxide) (PEO) based co-polymer. The battery also consisted of metallic Li and a charged cathode material. The battery operating temperature was above ambient around 90 °C to promote the best Li-ion

conductivity in the polymer. Because the polymer was only oxidatively stable to about 3.9 V versus Li metal, low voltage cathode materials were required. One goal of the project was to develop alternative cathode materials to replace V_2O_5 which was the existing cathode material. V_2O_5 was found to undergo a phase change after the first discharge which affected its cycle performance. At Argonne, we synthesized and tested LiV_3O_8 and doped LiV_3O_8 as a new cathode material [19]. LiV_3O_8 may be regarded as a lithia (Li_2O) stabilized V_2O_5 compound. The equivalent composition is $Li_2O{\cdot}3V_2O_5$. LiV_3O_8 did provide greater initial capacities in the range of 280 mAh g^{-1} without phase changes, compared with about 220 mAh g^{-1} for V_2O_5. However, since vanadium oxide is a regulated hazardous chemical (Resource Conservation Recovery Act (RCRA); P-listed hazardous chemical, P120) [20], it was desirable to consider and test other materials consisting of a manganese based electrode. After some consideration, we decided to test alpha-MnO_2 materials as charged cathodes for the Li-polymer battery.

Alpha-MnO_2 (α-MnO_2) has a 2 × 2 tunnel structure whereby MnO_6 octahedra are corner and edged shared to form the tunnel in Fig. 1. Typically, and in nature, the tunnel contains a foreign cation such as K^+ (cryptomelane) or Ba^{2+} (hollandite) which functions to stabilize the tunnel. In early 1990s, it was found that α-MnO_2 could be synthesized without foreign cations in the tunnel, but a water molecule (H_2O) could be located in the tunnel [21]. A sizable amount of water could be located in the tunnel at approximately 21 wt%. The structure was determined from neutron diffraction [21]. α-MnO_2 may be synthesized from sulfuric acid-treatment of Mn_2O_3 (bixybite) at temperatures about 90–100 °C. The oxygen from the water molecule fits in the special position in the middle of the tunnel and approximates a distorted hcp oxygen array stacking sequence. The protons are hydrogen bonded to the walls of the tunnel and the walls are slightly pushed outward to accommodate the repulsion between oxide anions. It was key that the tunnel now could be stabilized by an anion instead of, typically, a cation.

The thermal stability of hydrated versus heat-treated α-MnO_2 cathode materials (3 V system) was measured. The amount of structurally incorporated water (2 × 2 tunnel H_2O) was determined to be α-$MnO_2{\cdot}0.15H_2O$ [22]. These α-MnO_2 products are thermally stable to approximately 490 °C, then convert in a two-step process to Mn_2O_3 at 700 °C, and a subsequent one-step process to Mn_3O_4 at 1000 °C in air. The hydrated form of α-MnO_2 can be dehydrated at 275 °C in air to form a heat-treated (HT) α-MnO_2 without anything within the 2 × 2 tunnel. The lattice parameter $a = b$ is typically about 9.75 Å for the HT α-MnO_2, whereas when the material is hydrated as α-$MnO_2{\cdot}0.15H_2O$ the lattice expands to around 9.81 Å to accommodate H_2O in the tunnel [23]. HT α-MnO_2 is a powerful dessicant; it can reabsorb water in an exothermic process [24].

It was hypothesized that it may be possible to replace the water (H_2O) molecule with a lithium oxide molecule (Li_2O) to essentially create a lithia-stabilized α-MnO_2 with an identical structure. A hydrated form of α-MnO_2 is intimately mixed with lithium-hydroxide in methanol. After drying, the mix is fired at low temperatures about 300 °C to promote reaction and substitution of the water molecule with Li_2O. Neutron diffraction was used to characterize the product: α-$[0.15Li_2O]{\cdot}MnO_2$. It was found that the Li_2O is positioned within the tunnel with the O^{2-} anion of Li_2O occupying the special position (0,0,0.4) with an occupancy of 0.20 [23]. Subsequent experiments were used to vary the quantity of Li_2O substitution and to follow the change in lattice parameter of the tetragonal unit cell (*I*4/*m*). In response to addition of Li_2O into the structure of α-MnO_2, the lattice expands in a linear trend consistent with Vegards Law of solid–solution behavior. Fig. 2 shows the change in $a = b$ lattice parameter where the net result is an expansion of the 2 × 2 tunnel dimension to accommodate increasing amounts of Li_2O. When the composition approaches Li/Mn = 0.5 or $0.25Li_2O{\cdot}MnO_2$, then a spinel phase begins to form in the matrix and the XRD pattern shows two phases, one is the lithia-stabilized α-MnO_2 and the other is the spinel, $LiMn_2O_4$.

The cycling performance of the lithia-stabilized α-MnO_2 is shown in Fig. 3. In this case the α-MnO_2 (heat-treated at 275 °C) and NH_3-treated analogs of lithia-stabilized α-MnO_2 and α-MnO_2 are compared. The ammonia treatment was found to improve the capacity stabilization [25]. Since α-MnO_2 and lithia-stabilized α-MnO_2 contain some nominal amount of water in the material, it was hypothesized that low-temperature treatment with ammonia gas could be used to replace the water. Ammonia (NH_3) is very similar in property to water (H_2O); both form hydrogen bonds and have a similar molecular size

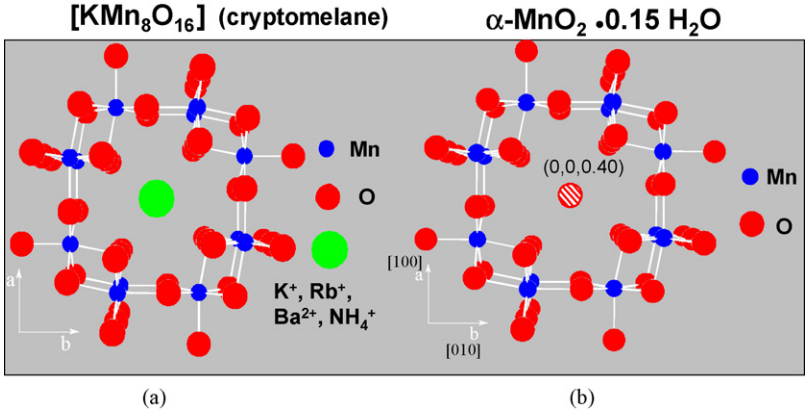

Fig. 1. Schematic structural representation of 2 × 2 tunnel structures of MnO_2: (a) cryptomelane, KMn_8O_{16}, and (b) hydrated α-$MnO_2{\cdot}0.15H_2O$.

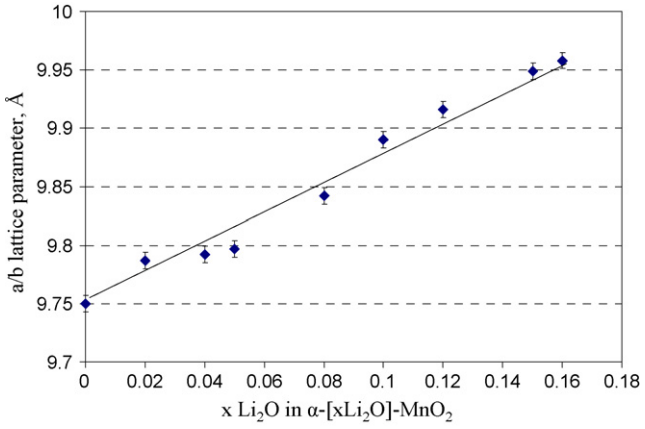

Fig. 2. α-MnO_2 lattice parameter change as a function of addition of x lithia (Li_2O) to the α-MnO_2 structure: α-[xLi_2O]·MnO_2.

[26]. NH_3 may react with protons in the MnO_2 materials to form ammonium cations (NH_4^+) which can stabilize the 2 × 2 tunnel structure thereby improving the cycling performance.

The stability of NH_3-treated, Li_2O-stabilized α-MnO_2 provides the highest rechargeable capacity and is above 220 mAh g^{-1} at 20 cycles when charged and discharged between 3.8 and 2.0 V. Other comparative materials show greater fade. Such a stable large capacity supports the fact that Li_2O-stabilized α-MnO_2 can provide energy densities above 500 Wh kg^{-1} (Table 1). The voltage profile is provided in Fig. 4; the discharge curve for the first discharge and the 40th discharge are plotted. Note that the profile involves two plateaus for reaction or insertion of Li which suggests that two inequivalent sites are available to place lithium. The plateaus are higher in voltage on the 40th discharge cycle which suggests that a decrease in the cell impedance occurs during cycling. This two-step process has been observed previously in cyclic voltammetric studies of α-MnO_2 [21]. It is likely that the Li first inserts into the 2 × 2 tunnel coordinating with the Li_2O tunnel oxygen anion and the O^{2-} anions along the walls. Effectively there are four equivalent positions to coordinate Li^+. Once the first Li is introduced, then

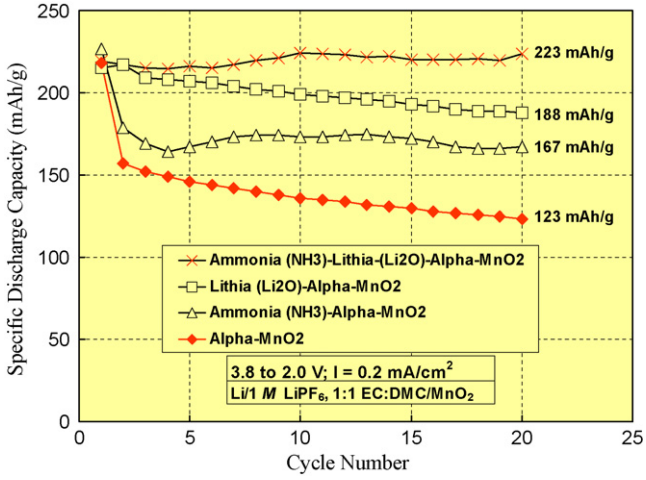

Fig. 3. Discharge capacity (mAh g^{-1}) vs. cycle number for a series of α-MnO_2 electrode materials.

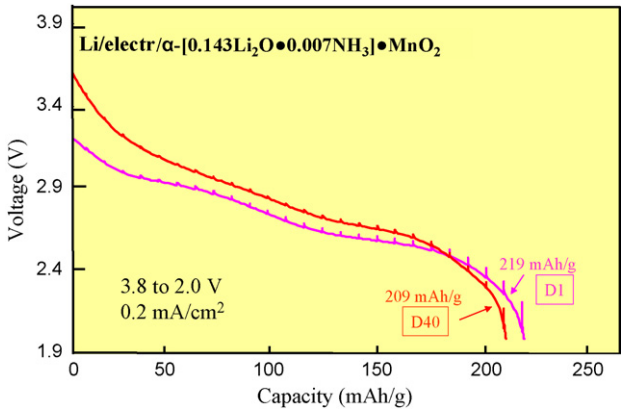

Fig. 4. Galvanostatic discharge voltage profiles of Li/α-[0.143Li_2O·0.007NH_3]·MnO_2 cell. The voltage spikes are due to current interruptions taken every 30 min.

it is probable that the next Li inserts in the opposite corner to the first lithium. More experiments will be necessary to unequivocally assign the positions that Li resides in a discharged material.

2.3. *Layered–layered composite structures from Li_2MnO_3*

Despite considerable effort to develop a layered $LiMnO_2$-type structure over several years, the electrochemical performance of these layered materials has not yet been sufficiently good enough to challenge the performance of manganese spinel or layered $LiCoO_2$ electrodes, the latter material being the most widely commercialized. With the recent publications of the successful synthesis of layered $LiNi_{1/2}Mn_{1/2}O_2$, and $LiNi_{1/3}Mn_{1/3}Co_{1/3}O_2$ compounds that are isostructural with $LiCoO_2$, renewed attempts are being made to develop a layered manganese electrode that may be competitive to $LiCoO_2$. This section puts the development of layered manganese oxides into perspective and highlights future and potentially exciting opportunities for developing a layered lithium-manganese-oxide material consisting of a composite electrode structure of $xLi_2MnO_3·(1-x)LiMO_2$ (where M = Mn, Ni and/or Co) as an alternative to $LiCoO_2$.

A series of compounds with a general formula $Li_{2-y}MnO_{3-y/2}$ ($0 < y < 2$) were prepared from acid-leaching lithia (Li_2O) from rock salt Li_2MnO_3 [27,28]. This process is typically done at room temperature in 2 M sulfuric acid. Proton exchange with lithium cations first occurs, then lithia (Li_2O) from the interlayer space of Li_2MnO_3 ($Li[Li_{0.33}Mn_{0.67}]O_2$) is removed by a displacement of O^{2-} and Li^+ diffusion along the b-axis of the Li_2MnO_3 C2/c unit cell. A structural refinement (monoclinic system) of the acid-leached products indicates shrinkage in the c-axis unit cell [29].

This reaction was found to be a two-phase reaction such that a cooperative shearing mechanism was occurring. Li-6 solid-state NMR results were used to probe the reaction mechanism [30]. Fig. 5 contains results from an experiment wherein a new phase grows while the parent original Li_2MnO_3 phase disappears in an equivalent manner. In trace (a), we see three signals or peaks for Li_2MnO_3 parent material one of which can be assigned to Li in

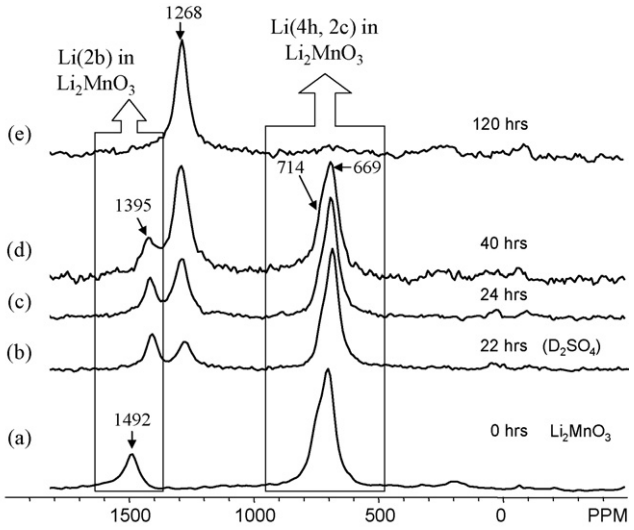

Fig. 5. Solid-state MAS Li-6 NMR of: (a) starting material Li_2MnO_3, (b) Li_2MnO_3 after 22 h acid-leaching in 2.5 M D_2SO_4, (c) Li_2MnO_3 after 24 h acid-leaching in 2.5 M D_2SO_4, (d) Li_2MnO_3 after 40 h acid-leaching in 2.5 M D_2SO_4, (e) Li_2MnO_3 after 120 h acid-leaching in 2.5 M D_2SO_4.

the transition metal layers (Li (2b)), and two inequivalent signals due to Li in the Li-layers (Li (4h) and Li (2c)). As the material is subjected to acid over time Li_2O is leached out of the structure and a new peak due to new Li in the sheared *P*3 prismatic phase starts to grow positioned at 1268 ppm. Note that the shift in the 2b resonance of Li_2MnO_3 from 1492 to 1395 ppm when subjected to acid is due to slightly different experimental conditions used to acquire the spectra. Effectively the 1395 ppm resonance is also due to 2b Li sites. In the final trace (e), the resultant product contains very little Li_2MnO_3 (<1.4 wt.%) and is mostly the new prismatic phase with the proton exchanged composition $H[Li_{0.33}Mn_{0.67}]O_2$. Thermogravimetric analysis on the weight loss on decomposition of $H[Li_{0.33}Mn_{0.67}]O_2$ agrees with results on the H-content by proton (deuteron) NMR [30]. The following Eqs. (1)–(3) describe the ion-exchange of H^+ for Li^+ and the acid-leaching of Li_2O. Residual Li_2MnO_3 is written in brackets in the equation in order to represent the portion of the material that is retained as Li_2MnO_3. In addition Li_2MnO_3 is rewritten in layered notation ($Li(Li_{0.33}Mn_{0.67})O_2$) to highlight the H for Li exchange in the Li-layers.

$$[Li(Li_{0.33}Mn_{0.67})O_2] + x\delta H^+ \rightarrow 1-x[Li(Li_{0.33}Mn_{0.67})O_2]\cdot x[Li_{1-\delta}H_\delta(Li_{0.33}Mn_{0.67})O_2] + x\delta Li^+ \quad (1)$$

Here δ represents the amount of protons exchanged for lithium cations in formation of the new phase, $Li_{1-\delta}H_\delta(Li_{0.33}Mn_{0.67})O_2$. The coefficient x is the quantity of the new phase formed in acid. Continued reaction causes a net amount of lithium oxide to be leached out of the material and this reaction is depicted in Eq. (2). In addition, the structural protons are stripped away as evolved water.

$$1-x[Li(Li_{0.33}Mn_{0.67})O_2]\cdot x[Li_{1-\delta}H_\delta(Li_{0.33}Mn_{0.67})O_2] \rightarrow 1-x[Li(Li_{0.33}Mn_{0.67})O_2]\cdot x[0.67MnO_2] + x(0.665-\delta/2)Li_2O + x(\delta/2)H_2O \quad (2)$$

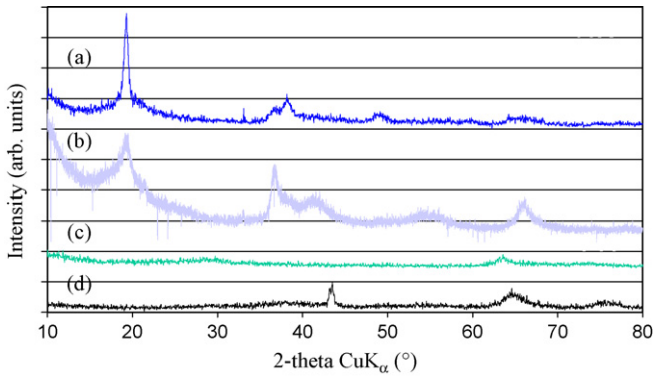

Fig. 6. Powder X-ray diffraction patterns for: (a) acid-leached Li_2MnO_3; $1-x[Li(Li_{0.33}Mn_{0.67})O_2]\cdot x$ [$0.67MnO_2$], measured on 3/95, (b) sample from (a) measured on 10/97, (c) sample from (a) measured on 3/98, and (d), material from (a), but mixed with and in contact with carbon powder.

The product that is formed consists of a 'composite' structure of $1-x[Li(Li_{0.33}Mn_{0.67})O_2]\cdot x[0.67MnO_2]$ or written in another form simply as $(1-x)Li_2MnO_3\cdot xMnO_2$. The MnO_2 portion has a layered structure where the oxygen close-packed lattice is structurally integrated or bonded with the Li_2MnO_3 portion.

This material, $1-x[Li(Li_{0.33}Mn_{0.67})O2]\cdot x[0.67MnO_2]$, is a "charged" electrode, thus it may be discharged first for application in a metallic Li secondary battery (rechargeable Li-polymer cell) or as a cathode in primary lithium cells. When cycled in a Li button cell, the acid-leached product gave 155 mAh g^{-1} capacity on the 12th cycle (C/15 rate; 3.8–2.0 V) [29]. The electrochemical profile suggests that the material does not convert to a spinel during cycling. However, it appears that the structure does slowly convert to an amorphous MnO_2 (Fig. 6, pattern c). The material loses crystallinity and broad humps in the X-ray diffraction develop on standing (Fig. 6, pattern b). This process seems to be accelerated if the powder is either (a) kept in contact with carbon powder (i.e. laminate mix, Fig. 6, pattern d), or (b) not kept very dry, for instance, not stored in a vacuum dessicator. Apparently, residual water in the structure may play a role in the interconversion mechanism.

A subsequent chemical lithiation (LiI) or electrochemical Li insertion (initial discharge) (Eq. (3)) can been used to reinsert lithium without any shear of the structure. This process is, in effect, a way to synthesize a "discharged" cathode. Because Li cannot be inserted into Li_2MnO_3 (or $Li[Li_{0.33}Mn_{0.67}]O_2$), then it inserts into the layered MnO_2 portion of the composite.

$$1-x[Li(Li_{0.33}Mn_{0.67})O_2]\cdot x[0.67MnO_2] + (0.67)xzLi \rightarrow 1-x[Li(Li_{0.33}Mn_{0.67})O_2]\cdot x[0.67Li_zMnO_2] \quad (3)$$

The material $1-x[Li(Li_{0.33}Mn_{0.67})O_2]\cdot x[0.67Li_zMnO_2]$, therefore, represents a mixed-valent composite-structured electrode consisting of Mn(IV) in the Li_2MnO_3 portion of the composite and Mn(III) in the $LiMnO_2$ portion of the composite. This concept can be extended to other Mn(IV)/Mn(III) ratios where one can represent the composite with rock-salt notation of $Li_aMn_bO_c$ where $a+b=c$. Table 2 shows some representative compositional relationships in the pure Mn system such as "$Li_3Mn_2O_5$", which is 50% Li_2MnO_3 and 50% $LiMnO_2$.

Table 2
Compositional relationships for pure Mn-oxide systems: $[xLi_2MnO_3\cdot(1-x)LiMnO_2]$

x	1	0.67	0.5	0.33	0
% Mn(IV)	100	67	50	33	0
% Mn(III)	0	33	50	67	100
Rock salt notation	Li_2MnO_3	$Li_5Mn_3O_8$	$Li_3Mn_2O_5$	$Li_4Mn_3O_7$	$LiMnO_2$
Theoretical capacity (mAh g^{-1})	0	82	127	176	286

Other compositions can be formulated as "$Li_5Mn_3O_8$" which is Li_2MnO_3 rich (67%) or "$Li_4Mn_3O_7$" which is $LiMnO_2$ rich (67%). The portion of the material that is electrochemically active between 4.5 and 2.0 would be the $LiMnO_2$ part of the composite. Note that it has also been demonstrated that Li_2MnO_3 may be activated electrochemically at high voltages (>4.5 V) [31,32] or from acid-treatment [27–29]. The theoretical capacities are listed in Table 2. Capacities are from the $LiMnO_2$ part of the composite for cycling below 4.5 V.

Now, taking the "$Li_5Mn_3O_8$" composition and highlighting the individual oxidation states of the Mn leaves the composition "$Li_5Mn_2^{IV}Mn^{III}O_8$": one-third of the Mn metal in the material consists of Mn(III). Rewriting "$Li_5Mn_2^{IV}Mn^{III}O_8$" in composite notation yields a discharged $0.67Li_2MnO_3\cdot0.33LiMnO_2$ electrode (i.e. one within the $xLi_2MnO_3\cdot(1-x)LiMnO_2$ family of compounds). This notation formed the basis for so-called layered–layered 'composite' structures as proposed by Johnson and Thackeray [17]. This concept was subsequently used to design a new family of $(1-x)Li_2M'O_3\cdot xLiMO_2$ electrodes with structurally compatible components that could be synthesized in the discharged state, where M′ is a collection of transition metals with an average oxidation state of IV, and M is a collection of transition metals with an average oxidation state of III, for example, $0.05Li_2TiO_3\cdot0.95Li(Mn_{0.5}Ni_{0.5})O_2$ reported by Kim et al. [33] and Johnson et al. [34]. Similar compositions containing Cr and Co as M cations and Mn as M′ cations were reported by Ammundsen et al. [35] and Numata et al. [36] respectively. More recently Zhang et al. [37], Kim et al. [38], and Whitfield et al. [39] studied the synthesis, characterization and electrochemistry of the electrodes, written in composite notation, $Li_2MnO_3\cdot LiNiO_2$, $Li_2MnO_3\cdot Li(Mn_{0.5}Ni_{0.5})O_2$, and $Li_2MnO_3\cdot Li(Ni_{1-x}Co_x)O_2$, respectively. The likelihood of the layered–layered composite structures to form, is due to the tendency of Mn(IV) to form Li_2MnO_3-like clusters in the presence of extra amounts of Li. Indeed, an ordering peak, indexed as the (0 2 0) monoclinic (*C*2/*m*) reflection that occurs around 22° 2-theta may be observed in such XRD patterns. Fig. 7 is a representative composition $0.5Li_2MnO_3\cdot0.5Li(MnNiCo)_{1/3}O_2$ where a small peak at ~22° is clearly observed in the pattern (marked with an arrow). In Li_2MnO_3 this peak occurs because the presence of extra monovalent lithium cations in the transition metal M layer that causes an ordering of Mn in that layer. As more Li and Mn are added to the system, the Li_2MnO_3-like character increases in the material. HRTEM and NMR studies on $(1-x)Li_2MnO_3\cdot xLi(Mn_{0.5}Ni_{0.5})O_2$ structures that contain M = Ni + Mn have confirmed the existence of such Li_2MnO_3-like clusters [40]. Further information on 'layered–layered' composites and 'layered-spinel' composite structures can be found in a recent review paper by Thackeray et al. [18].

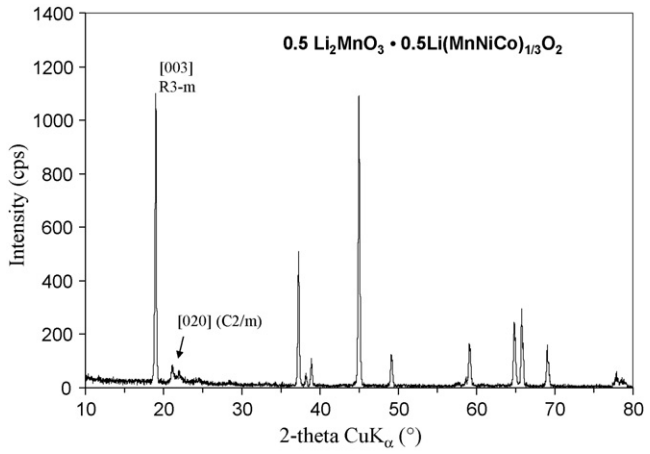

Fig. 7. Powder X-ray diffraction pattern for layered–layered composite $0.5Li_2MnO_3\cdot0.5Li(MnNiCo)_{1/3}O_2$.

3. Conclusions

α-MnO_2 when stabilized with Li_2O has shown promise as 3 V MnO_2 electrode material. MnO_2-type materials have a propensity to form molecular level intergrowths and composites. Gamma γ-MnO_2, the material used in alkaline batteries is an intergrowth. Intergrowths or composites can be extended to lithium-manganese oxides for lithium batteries with a focus on Li_2MnO_3 composite layered structures. These include layered oxide phases that are formulated as composite-structured electrodes. Layered–layered type $xLi_2MnO_3\cdot(1-x)LiMO_2$ (M = Ni, Co and/or Mn) and layered-spinel types $xLi_2MnO_3\cdot(1-x)Li_{1+\delta}M_{2-\delta}O_4$ (M = Ni, Co and/or Mn) [41] have been discovered and are under evaluation.

Acknowledgments

The author would like to thank the following individuals for helpful discussions on this work including Michael Thackeray, Clare Grey, Stephen Hackney and Jack Vaughey. Numerous colleagues and students must also be thanked for their efforts and support of the research discussed in this paper including Dennis Dees, Don Vissers, Jai Prakash, Andy Jansen, Yang Shao-Horn, Michael Mansuetto, Arthur Kahaian, Roy Benedek, A. Jeremy Kropf, Donald Ng, Keith Miller, Liam Noailles, Scott Korte, Todd Bofinger, Kevin Lauzze, Chrissy Lefief, Xiaoqing Qian, Sean Odeen, Brett Isselhardt, Nick Kanakaris, Marion Houliére, Nathanael Fackler, Phalali Motsoetsoe, Younkee Paik, Naichao Li and Jeom-Soo Kim. Financial support from the Office of Basic Energy Sciences and the Office of FreedomCar and Vehicle

Technologies of the U.S. Department of Energy under Contract No. W31-109-Eng-38 is gratefully acknowledged.

The submitted manuscript has been created by the University of Chicago as Operator of Argonne National Laboratory ("Argonne") under Contract No. W-31-109-ENG-38 with the U.S. Department of Energy. The U.S. Government retains for itself, and others acting on its behalf, a paid-up, non-exclusive, irrevocable worldwide license in said article to reproduce, prepare derivative works, distribute copies to the public, and perform publicly and display publicly, by or on behalf of the Government.

References

[1] S. Fritsch, A. Navrotsky, J. Am. Ceram. Soc. 79 (1996) 1761.
[2] D.D. MacNeil, Z. Lu, Z. Chen, J.R. Dahn, J. Power Sources 108 (2002) 8.
[3] N.N. Greenwood, A. Earnshaw, Chemistry of the Elements, first ed., Pergamon Press, Oxford, 1984, pp. 1212.
[4] M.M. Thackeray, Prog. Solid State Chem. 25 (1997) 1.
[5] D. Glover, B. Schumm Jr., A. Kozawa, Handbook of Manganese Oxides Battery Grade, first ed., International Battery Materials Association (IBA Inc.), Cleveland, 1989.
[6] M.M. Thackeray, A. DeKock, M.H. Rossouw, D. Liles, R. Bittihn, D. Hoge, J. Electrochem. Soc. 139 (1992) 363.
[7] M.M. Thackeray, M.H. Rossouw, A. DeKock, A.P. Delaharpe, R.J. Gummow, K. Pearce, D.C. Liles, J. Power Sources 43 (1993) 289.
[8] H. Ikeda, J. Power Sources 9 (1983) 329.
[9] T. Ohzuku, M. Kitagawa, T. Harai, J. Electrochem. Soc. 136 (1989) 3169.
[10] M.M. Thackeray, M.H. Rossouw, R.J. Gummow, D.C. Liles, K. Pearce, A. DeKock, W.I.F. David, S. Hull, Electrochim. Acta 38 (1993) 1259.
[11] W. Tang, S. Yang, S. Liu, K. Ooi, J. Mater. Chem. 13 (2003) 2989.
[12] D. Larcher, B. Gerand, J.M. Tarascon, Int. J. Inorg. Mater. 2 (2000) 389.
[13] T. Nohma, T. Saito, N. Furakawa, H. Ikeda, J. Power Sources 26 (1989) 389.
[14] Y. Paik, W. Bowden, T. Richards, C.P. Grey, J. Electrochem. Soc. 152 (2005) A1539.
[15] H. Nakamura, K. Motooka, H. Noguchi, M. Yoshio, J. Power Sources 81–82 (1999) 632.
[16] Y. Shao-Horn, S.A. Hackney, A.R. Armstrong, P.G. Bruce, R. Gitzendanner, C.S. Johnson, M.M. Thackeray, J. Electrochem. Soc. 146 (1999) 2404.
[17] C.S. Johnson, M.M. Thackeray, in: A. Landgrebe, R.J. Klingler (Eds.), Interfaces, Phenomena, and Nanostructures in Lithium Batteries, Proceedings volume 2000-36, The Electrochemical Society Inc., Pennington, New Jersey, 2001, p. 47.
[18] M.M. Thackeray, C.S. Johnson, J.T. Vaughey, N. Li, S.A. Hackney, J. Mater. Chem. 15 (2005) 2257.
[19] M. M. Thackeray; A. Kahaian, K. Kepler, D. Vissers, U.S. Patent number 6,322,928.
[20] http://www.epa.gov/rcraonline/.
[21] M.H. Rossouw, D.C. Liles, M.M. Thackeray, W.I.F. David, S. Hull, Mater. Res. Bull. 27 (1992) 221.
[22] Y. Shao-Horn, S.A. Hackney, C.S. Johnson, M.M. Thackeray, J. Electrochem. Soc. 145 (1998) 582.
[23] C.S. Johnson, D.W. Dees, M.F. Mansuetto, M.M. Thackeray, D.R. Vissers, D. Argyiou, C.-K. Loong, L. Christensen, J. Power Sources 68 (1997) 570; C.S. Johnson, D.W. Dees, M.F. Mansuetto, M.M. Thackeray, D.R. Vissers, D. Argyiou, C.-K. Loong, L. Christensen, J. Power Sources 75 (1998) 183.
[24] C.S. Johnson, unpublished results, 1995.
[25] C.S. Johnson, M.M. Thackeray, J. Power Sources 97–98 (2001) 437.
[26] F.A. Cotton, G. Wilkinson, Advanced Inorganic Chemistry: A Comprehensive Text, fourth ed., John Wiley & Sons, New York, 1980, pp. 414–416.
[27] M.H. Rossouw, M.M. Thackeray, Mater. Res. Bull. 26 (1991) 463.
[28] M.H. Rossouw, D.C. Liles, M.M. Thackeray, J. Solid State Chem. 104 (1993) 464.
[29] C.S. Johnson, S.D. Korte, J.T. Vaughey, M.M. Thackeray, T.E. Bofinger, Y. Shao-Horn, S.A. Hackney, J. Power Sources 81 (1999) 491.
[30] Y. Paik, C.P. Grey, C.S. Johnson, J.-S. Kim, M.M. Thackeray, Chem. Mater. 14 (2002) 5109.
[31] C.S. Johnson, J.-S. Kim, C. Lefief, N. Li, J.T. Vaughey, M.M. Thackeray, Electrochem. Commun. 6 (2004) 1085.
[32] A.D. Robertson, P.G. Bruce, Chem. Mater. 15 (2003) 1984.
[33] J.-S. Kim, C.S. Johnson, M.M. Thackeray, Electrochem. Commun. 4 (2002) 205–209.
[34] C.S. Johnson, J.-S. Kim, A.J. Kropf, A.J. Kahaian, J.T. Vaughey, M.M. Thackeray, J. Power Sources 119 (2003) 139.
[35] B. Ammundsen, J. Paulsen, I. Davidson, R.-S. Liu, C.-H. Shen, J.-M. Chen, L.-Y. Jang, J.-F. Lee, J. Electrochem. Soc. 149 (2002) A431.
[36] K. Numata, C. Sakaki, S. Yamanaka, Solid State Ionics 117 (1999) 257.
[37] L.Q. Zhang, H. Noguchi, M. Yoshio, J. Power Sources 110 (2002) 57.
[38] J.-S. Kim, C.S. Johnson, M.M. Thackeray, Electrochem. Commun. 4 (2002) 205.
[39] P.S. Whitfield, S. Niketic, I.J. Davidson, J. Power Sources 146 (2005) 617.
[40] J.-S. Kim, C.S. Johnson, J.T. Vaughey, M.M. Thackeray, W. Yoon, C.P. Grey, Chem. Mater. 16 (2004) 1996.
[41] C.S. Johnson, N. Li, J.T. Vaughey, M.M. Thackeray, Electrochem. Commun. 7 (2005) 528.